

Trends and uncertainties in Siberian indicators of 20 century warming

by Jan Esper, David Frank, Ulf Büntgen, Anne Verstege

Rashit M. Hantemirov, Alexander Kirilyanov

Tree-ring data

The study area encompasses most of the plains and plateaus of Siberia including the Putorana and Chersky Mountains roughly separating western from eastern and northeastern Siberia. The area represents a significant portion of the circumpolar dendroclimatological dataset collected in the early 1990's by F.H. Schweingruber and colleagues including tree-ring width (TRW) and maximum latewood density (MXD) measurements (Schweingruber, 1993). The same data have previously been used to reconstruct spatial temperature patterns associated with pre-instrumental volcanic events (Briffa et al., 1998a), and to identify DP over larger regions (Briffa et al., 1998b). Generally, MXD derived timeseries correlate better than TRW with temperatures, contain less serial correlation -- i.e. are better high frequency indicators of summer temperature -- but might also be limited in reconstructing low frequency, multi-centennial climatic trends when using material from only living trees (Frank & Esper, 2005a, 2005b).

Tables S1 and S2 provide detail on the tree-ring clusters 1, 2, ...7 and the 78 site chronologies used in this study. The mean interseries correlation (Rbar) is a widely used measure of the internal coherence of tree-ring data (Cook and Kairiukstis, 1990). Higher Rbar scores often indicate datasets contain a stronger climatic signal. Measures of the lag-1 autocorrelation (AC(1)) are generally higher for TRW than MXD, and provide an idea of the memory or persistence of tree-ring timeseries. The 78 site records listed in Table S2 are a subset of all 97 datasets available in the study region. 19 of these datasets were discarded due to length requirements, i.e. records that start did not span the 1800 to 1970 period, or obvious lack of correlation with neighboring chronologies.

Table S1 Tree-ring data statistics of clusters C1 to C7, their regional means C1-3 and C4-6, and the mean of all data C1-7. MTA is mean tree age, Rbar is mean interseries correlation, and AC(1) is first year autocorrelation. Rbar and AC(1) were derived from 32-year spline and RCS detrended data (since 1800 AD), respectively.

Cluster	No. Sites (Larch/Spruce/Pine)	Lon.	Lat.	No. Cores	MTA	Ring Density			Ring Width		
						Mean	Rbar	AC(1)	Mean	Rbar	AC(1)
C1	12 (4/5/3)	67	66	501	182	0.73	0.56	0.32	0.53	0.55	0.51
C2	13 (11/2/0)	80	67	587	185	0.79	0.65	0.08	0.59	0.64	0.47
C3	7 (4/2/1)	92	70	350	203	0.76	0.61	0.04	0.37	0.62	0.37
C1-3	32 (19/9/4)	80	68	1438	190	0.76	0.61	0.15	0.49	0.60	0.45
C4	10 (8/1/1)	111	70	402	220	0.74	0.62	0.12	0.33	0.62	0.23
C5	18 (18/0/0)	146	69	620	277	0.76	0.61	0.18	0.32	0.61	0.23
C6	11 (8/2/1)	138	65	319	245	0.84	0.41	0.36	0.41	0.45	0.39
C4-6	39 (34/3/2)	132	68	1341	247	0.78	0.55	0.22	0.35	0.56	0.28
C7	7 (7/0/0)	154	62	296	309	0.78	0.58	0.18	0.36	0.61	0.27
C1-7	78 (60/12/6)	113	67	3075	232	0.77	0.58	0.18	0.41	0.59	0.35

30 *Climate data*

31 Two versions of monthly station temperatures were considered: the raw and adjusted data of the Global Historical
 32 Climatology Network (GHCN; Peterson et al., 1997), also available via the Royal Netherlands Meteorological
 33 Institute (KNMI; Oldenborgh et al., 2003). Considering these data, we calculated monthly anomalies with respect to
 34 the 1951-1980 period, computed mean JJA timeseries for each of the 13 stations, averaged these records for the 6
 35 WSIB, 5 ESIB, and 2 NESIB stations, and used the raw GHCN data for tree-ring calibration.

36 Table S3 provides detail on the 13 Siberian climate stations that started operating before 1910. The 1900-90 trends
 37 were obtained by fitting linear regressions lines to unadjusted JJA mean temperature timeseries. Inhabitant statistics
 38 were obtained from various Russian online resources.

39

40 **Table S3** Siberian long-term climate stations.

	Station	Lat.	Lon.	Period	1900–90 Trends	Population (Year)	
WSIB	1 Berezovo	63.9	65.0	1881–1990	0.27	1,400 (1897)	6,700 (2002)
	2 Salehard	66.5	66.7	1882–now	-0.13	500 (1897)	40,000 (2007)
	3 Hanty-Mansijs	61.0	69.0	1892–now	0.18	7,500 (1939)	63,200 (2007)
	4 Surgut	61.2	73.5	1884–1985	0.54	1,100 (1897)	289,900 (2007)
	5 Dudinka	69.4	86.2	1906–1990	0.81	80 (1926)	26,800 (2000)
	6 Turuhansk	65.8	87.9	1881–now	0.65	212 (1897)	4,800 (2002)
ESIB	7 Olekminsk	60.4	120.4	1882–1990	-1.71	1,144 (1897)	10,003 (2002)
	8 Viljujsk	63.8	121.6	1898–now	-0.05	600 (1897)	10,000 (2002)
	9 Jakutsk	62.0	129.7	1829–now	0.20	6,500 (1897)	246,000 (2007)
	10 Verhojansk	67.5	133.4	1885–now	-0.13	400 (1897)	1,300 (2007)
	11 Ust'-Maja	60.4	134.4	1893–1990	-0.51	—	3,800 (1999)
NESIB	12 Markovo	64.7	170.4	1894–1990	0.33	—	600 (2000)
	13 Anadyr'	64.8	177.6	1898–now	0.55	200 (1927)	11,900 (2000)

41

42

43 *Detrending and chronology building*

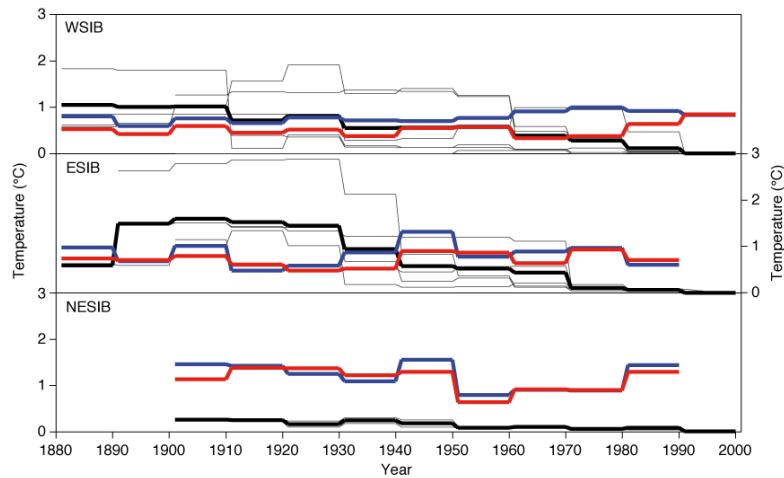
44 We applied four detrending methods, RCS, HUG, EXP, and SPL, to the single TRW and MXD measurement series
 45 by calculating ratios (residuals for HUG; Briffa et al. 1998) between the raw data and fitted growth curves. For each
 46 method, detrended series were averaged per site using a robust bi-weight mean and the variance of the mean
 47 chronologies' stabilized for changes in sample replication and interseries correlation (Frank et al., 2007).
 48 Chronologies were truncated over the 1801-1990 common period (1801-2000 for the WSIB update), and
 49 subsequently averaged to form the mean cluster chronologies (C1, C2, ..., C7). RCS was applied on a site-by-site
 50 basis (Esper et al., 2007), and the mean of all age-aligned data (i.e., the Regional Curve) smoothed using a 10-year
 51 spline (details in Esper et al., 2003). HUG included growth curve functions with positive slopes; EXP excluded such
 52 functions but utilized the long-term mean instead. SPL included the application of a cubic smoothing spline with a
 53 50% frequency-response cutoff for 300-year waveforms (details in Cook and Peters, 1981).

54

55 *Regional residual timeseries*

56 Figure S1 provides detail on the instrumental and proxy residuals in WSIB, ESIB, and NESIB (see main text for a
 57 description of residual calculation). Residuals were of similar size in WSIB and ESIB, including changes from about
 58 1°C to 0°C over the past century. In NESIB, where the proxy/temperature fit was weaker and the station data
 59 adjustments smaller, proxy residuals were about an order of magnitude larger than temperature residuals. As these

60 differences were biased by the greater distance between proxy and temperature sites, the NESIB data were not
61 included in the comparison as shown in Fig. 9 of the main text.



62

63 **Fig. S1** Decadally averaged residuals of the raw *versus* adjusted JJA temperature data (black), the MXD *versus*
64 JJA temperature data (red), and the TRW *versus* JJA temperature data (blue).

65

66 *References*

67 Briffa KR, Jones PD, Schweingruber FH, Osborn TJ (1998a) Influence of volcanic eruptions on Northern
68 Hemisphere summer temperature over the past 600 years. *Nature*, **393**, 450-455.

69 Briffa KR, Schweingruber FH, Jones PD, Osborn TJ, Shiyatov SG, Vaganov EA. (1998b). Reduced sensitivity of
70 recent tree-growth to temperature at high northern latitudes. *Nature*, **391**, 678-682.

71 Cook ER, Peters K (1981) The smoothing spline: a new approach to standardizing forest interior tree-ring width
72 series for dendroclimatic studies. *Tree-Ring Bulletin*, **41**, 45-53.

73 Cook ER, Kairiukstis LA (1990) *Methods of dendrochronology – applications in the environmental science*.
74 Kluwer, Dordrecht.

75 Esper J, Cook ER, Krusic PJ, Peters K, Schweingruber FH (2003) Tests of the RCS method for preserving low-
76 frequency variability in long tree-ring chronologies. *Tree-Ring Research*, **59**, 81-98.

77 Esper J, Frank DC, Wilson RJS, Büntgen U, Treydte K (2007) Uniform growth trends among central Asian low and
78 high elevation juniper tree sites. *Trees*, **21**, 141–150.

79 Frank D, Esper J (2005a) Characterization and climate response patterns of a high-elevation, multi-species tree-ring
80 network for the European Alps. *Dendrochronologia*, **22**, 107-121.

81 Frank D, Esper J (2005b) Temperature reconstructions and comparisons with instrumental data from a tree-ring
82 network for the European Alps. *International Journal of Climatology*, **25**, 1437-1454.

83 Frank D, Esper J, Cook ER (2007) Adjustment for proxy number and coherence in a large-scale temperature
84 reconstruction. *Geophysical Research Letters*, **34**, doi: 10.1029/2007GL030571.

- 85 Oldenborgh GJ van, Ulden A. van (2003) On the relationship between global warming, local warming in the
86 Netherlands and changes in circulation in the 20th century. *International Journal of Climatology*, **23**, 1711-1723.
- 87 Peterson TC, Vose RS (1997) An overview of the Global Historical Climatology Network temperature database.
88 *Bulletin of the American Meteorological Society*, **78**, 2837-2849.
- 89 Schweingruber FH, Bräker OU, Schär E (1979) Dendroclimatic studies on conifers from central Europe and Great
90 Britain. *Boreas*, **8**, 427-452.
- 91 Schweingruber FH (1993) Dendrochronological sampling strategies for radiodensitometric networks in northern
92 hemisphere subalpine and boreal zones. *European Palaeoclimate and Man*, **4**, 205-209.